Applied Physics Letters

RESEARCH ARTICLE | AUGUST 07 2023

Atomic layer etching (ALE) of III-nitrides

Wan Ying Ho; Yi Chao Chow; Zachary Biegler; Kai Shek Qwah; Tanay Tak; Ashley Wissel-Garcia; Iris Liu; Feng Wu; Shuji Nakamura; James S. Speck

Appl. Phys. Lett. 123, 062102 (2023)
https://doi.org/10.1063/5.0159048

Atomic layer etching (ALE) of III-nitrides

Cite as: Appl. Phys. Lett. **123**, 062102 (2023); doi: 10.1063/5.0159048
Submitted: 19 May 2023 · Accepted: 27 July 2023 ·
Published Online: 7 August 2023

Wan Ying Ho,[1,a)] Yi Chao Chow,[1] Zachary Biegler,[1] Kai Shek Qwah,[1] Tanay Tak,[1] Ashley Wissel-Garcia,[1] Iris Liu,[1] Feng Wu,[1] Shuji Nakamura,[1,2] and James S. Speck[1]

AFFILIATIONS

[1]Materials Department, University of California, Santa Barbara, California 93106-5050, USA
[2]Department of Electrical and Computer Engineering, University of California, Santa Barbara, California 93106-5050, USA

[a)]Author to whom correspondence should be addressed: wanying_ho@ucsb.edu

ABSTRACT

Atomic layer etching (ALE) was performed on (Al, In, Ga)N thin films using a cyclic process of alternating Cl_2 gas absorption and Ar^+ ion bombardment in an inductively coupled plasma etcher system. The etch damage was characterized by comparing photoluminescence of blue single quantum well light-emitting diodes before and after the etch as well as bulk resistivities of etched *p*-doped layers. It was found that etched surfaces were smooth and highly conformal, retaining the step-terrace features of the as-grown surface, thus realizing ALE. Longer exposures to the dry etching increased the bulk resistivity of etched surfaces layers slightly, with a damaged depth of $\sim$55 nm. With further optimization and damage recovery, ALE is a promising candidate for controlled etching with atomic accuracy. It was found that $Al_{0.1}Ga_{0.9}N$ acts as an etch barrier for the ALE etch, making it a suitable etch to reveal buried V-defects in III-nitride light emitting diodes.

Group III nitrides (III-N) are important semiconductors forming the basis of light-emitting diodes (LEDs) and are gaining traction for use in power electronics, which applications extend from display technologies, communications to electric vehicles. One of the major roadblocks to III-N device design and fabrication is the lack of a wet etchant for Ga-face *c*-plane GaN, which is the dominant growth crystal plane of most GaN-based thin films.[1–3] While various low damage photoelectrochemical (PEC) etching techniques have been reported for Ga-face *c*-plane GaN, the resultant etched surfaces tend to be rough with formation of whiskers and etched pits.[1,4–7] Hence, there is need to develop low damage dry plasma etching techniques to enable device fabrication on III-nitrides, such as atomic layer etching (ALE). The technology of ALE dates to 1990, when the first ALE etching of Si was demonstrated.[8] ALE of GaAs was first reported in 1996,[9] Ge in 1997,[10] and GaN in 2002.[11]

For ALE etching of GaN, etching is usually achieved by first dosing the sample surface with Cl_2 gas, with which Cl adsorbs onto the dangling bonds of the material surface.[12–15] This step lowers the energy required for subsequent desorption of the Cl-terminated top layer—presumably either in the form of GaCl or $GaCl_3$.[15,16] The nitrogen atoms are desorbed as nitrogen gas, N_2.[16] Once the surface is saturated with chlorine, the chamber was evacuated. In the third step, the energy required for such desorption is provided typically by an Ar^+ ion plasma. The chamber is once again pumped down in preparation for the next cycle. However, the technology for GaN is far from maturity—with most recent publications reporting some form of damage to the etched surface or sidewalls.[13,14,16] Fukumizu *et al.* observed degradation of near band edge emission of the AlGaN surface layer etched using Cl_2/Ar ALE chemistry, with the increased damage for increased exposure to the Ar plasma.[13] Ruel *et al.* reported degradation of sheet resistance of the etched surface. They also reported recovery using additional N_2 annealing.[14]

The following work discusses the various characterization performed to justify or disqualify use of present ALE technology for surface sensitive devices, as well as microscopic and spectroscopic studies, such as electron emission spectroscopy (EES), electron emission microscopy (EEM), and photoemission spectroscopy (PES).[17–20] First, the degree of etch damage affects the emitting surface and transport properties. Second, the etch damage will modify transport properties throughout the damaged region—introducing scattering centers and altering diffusion lengths. If the damage depth is large, it also places an upper limit on etch depth, as further etches will result in damage to the active region in optoelectronic devices, altering the devices altogether.

An Oxford PlasmaPro 100 Cobra, an inductively coupled plasma (ICP) etcher with ALE capabilities, was used for the studies.[21] The ALE process used Cl_2 as the adsorption gas and Ar^+ as the sputtering ion source, with the parameters listed in Table I as recommended by the supplier.[21]

We note that the self-bias voltage during the Ar^+ etch step was 15 V. The chamber undergoes a long 30 min Cl_2/O_2 plasma clean and

TABLE I. The conditions during atomic layer etching in the Oxford PlasmaPro 100 Cobra.

Cl_2 Dose	Exposure time (t_{Cl})	0.04 s
	Chamber pressure (P_{Cl})	15 mTorr
	Cl_2 flow rate	50 sccm
Cl_2 Exhaust	Exhaust time	8.00 s
Ar^+ Etch	Exposure time (t_{Ar})	3.50 s
	Chamber pressure (P_{Ar})	10 mTorr
	ICP Power	500 W
	Ar flow rate	100 sccm
	Forward Bias Power	10 W
Ar^+ Exhaust	Exhaust time	1.50 s

a 50-cycle ALE conditioning run prior to etch. Samples ranging from sizes 5×5 to 10×10 mm^2 were mounted onto a 100 mm roughened sapphire carrier wafer using Santovac vacuum oil. The carrier was held at 20 °C through liquid nitrogen cooling.[21] Samples were dipped in buffered hydrofluoric acid (BHF) to remove surface oxides prior to introduction into the etching chamber.

For etch rate calibration, 100 nm of UID-GaN were grown on an AlGaN interlayer/GaN template/sapphire using ammonia molecular beam epitaxy (MBE) and plasma-assisted molecular beam epitaxy (PAMBE). The layer thicknesses are determined by measuring fringe spacing of the (0002) scan using x-ray diffraction (XRD) on a PANalytic MRD PRO diffractometer. A Seoul VioSys green multiple quantum-well (MQW) light-emitting diode (LED) sample was used to check for lithography compatibility of the technique. The sample was grown on a flat sapphire, with a pre-well InGaN/GaN superlattice (SL) structure, InGaN MQW with AlGaN cap and GaN quantum barrier (QB), and an AlGaN electron blocking layer (EBL). X-ray photoemission spectroscopy (XPS) was performed using a Thermo Scientific ESCALAB Xi+ x-ray photoelectron spectrometer microprobe on etched surfaces to determine the surface alloy composition by fitting Al 2p and Ga 3p peaks to obtain their respective atomic percentages. Atomic force microscopy (AFM) and scanning electron microscopy (SEM) were also performed on etched surfaces of the samples to characterize surface morphology and smoothness. For damage depth characterization, a blue $In_{0.15}Ga_{0.85}N$ single quantum-well (SQW) LED capped with 100 nm of UID-GaN was grown by metalorganic chemical vapor deposition (MOCVD). The sample was grown on a double side polished sapphire with the pre-well InGaN/GaN SL structure. Since the InGaN SQW disrupts the periodicity of the (000l) planes, clear thickness fringes in high resolution x-ray diffraction experiments can be attributed to the UID-GaN layer and, thus, the etch rate was also measured from the InGaN SQW sample. Two 150 nm *p*-GaN samples, one medium doped *p*-GaN ([Mg] $= 5 \times 10^{19}$ cm^{-3}) and one highly doped ([Mg] $= 2 \times 10^{20}$ cm^{-3}), were also grown on the single side polished sapphire using MOCVD for damage characterization using circular transmission line measurement (CTLM). The lower doped sample, henceforth referred to as MDp, corresponds to standard doping in the *p*-layer of an LED structure. The highly doped sample, henceforth referred to as HDp, corresponds to a typical highly doped *p*-contact layer. All grown samples were grown on the (0001) plane.

We found no significant differences in the etch rate per cycle between samples grown by different methods or doping, averaging at 2.7 Å/cycle indicating atomic layer etching [GaN atomic layer separation at 2.6 Å along the (0001) direction]. There was also no measured etch rate variation with sample size or location on the carrier wafer. With the etch rate per cycle reasonably consistent, we turn our attention to the damage resulting from the dry etch. If the ion bombardment introduced large amounts of lattice breaking and dangling bonds, we may observe a large change in surface morphology of the etched surfaces, either through formation of etch pits or significant roughening of the surface.[22,23] Atomic force microscopy (AFM) of etched ammonia MBE and PAMBE samples indicate that there is no added surface roughness, with the etch being mostly conformal, with a small smoothing effect at larger number of etch cycles. It is notable that no etched pits were introduced throughout the etch, which is commonly observed in etching of GaN as small hexagonal or circular depressions forming at the intersection of the dislocations and the sample surface.[24–26] The average roughness for $5 \times 5\,\mu$m^2 scans remains ~1 nm from pre-etch to post 225 etch cycles, as indicated in Fig. 1. The features remain similar after 50 and 225 etch cycles, with clearly defined step-terrace structure throughout the etch process and neither significant smoothing nor roughening taking place.

A deep hole was exposed on the PAMBE sample after 225 cycles of etching, which may be a previously buried extended defect in the sample. This hinted at the possibility of exposing filled-in V-defects in LEDs for V-defect characterization.[27,28] The etches were repeated on the Seoul VioSys multi-quantum well (MQW) sample, with lithographically defined squares to ensure lithography compatibility of the etch technique [see Fig. 2(a) inset for the epitaxial structure of the LED].

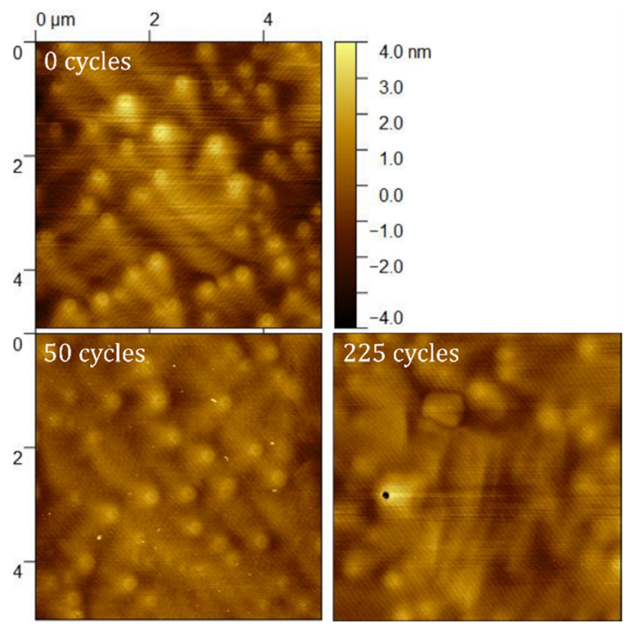

FIG. 1. AFM images of a PAMBE grown UID-GaN sample after different numbers of ALE cycles. The root mean squared roughness remains in ~1 nm, unchanged from unetched sample (0 cycles) to 225 cycle of etches. A deep hole was exposed after 225 cycles, which may be a previously buried defect in the sample.

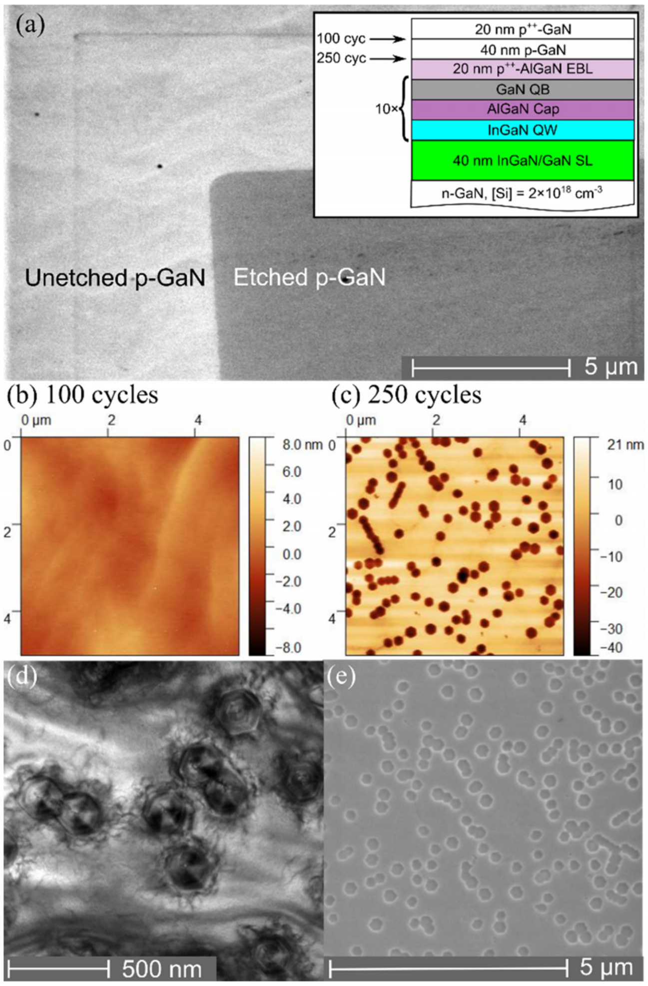

FIG. 2. At shallow etch depths (100 cycles, 22 nm etch depth), the etch was conformal and smooth as demonstrated by the SEM image in (a) and by AFM in (b). The epitaxial layer of the Seoul VioSys LED is depicted in inset of (a). At larger ALE etch cycle numbers (250 cycles), V-defects were exposed and is clearly resolved using AFM as seen in (c) as $Al_{0.1}Ga_{0.9}N$ acted as an etch barrier to ALE for the employed etch parameters. The V-defect density matched that measured in plan-view TEM in (d). In (e), the same etched surface as with (c) was imaged using SEM.

This is essential for devices where only lithographically exposed areas must be etched, such as etched-and-regrown gates in high-electron mobility transistors. As surface oxides serve as an etch barrier, we used SiO_x as a potential hard mask for the etch. For characterization of the etched surface, we employed SEM and AFM.

In Fig. 2(a), the etched surface at 22 nm etch depth as observed in SEM is smooth with no visible surface depressions, with clear patterning arising from the SiO_x hard mask etching only the exposed areas and ensuring its lithography compatibility. When a deeper etch was employed (150 cycles), it was observed that the etched surface was full of hexagonal shaped depressions (inverted hexagonal pyramids), which extended below and past the top quantum wells. Since such hexagonal shaped depressions were not observed in the AFM scans of etched ammonia MBE or PAMBE grown GaN samples, they cannot be etch pits due to the physical etch, and should be buried features already present in the unetched material. Further etches eventually prevented further removal of material, indicating presence of an etch stop layer. At 250 cycles of etch, a quick calculation using the $5 \times 5\,\mu m^2$ AFM scans in Fig. 2(c) indicated a density of 6×10^8 cm^{-3}, which corresponds well to the expected V-defect density of the wafer independently measured using plan view transmission electron microscopy (TEM) showed in Fig. 2(d). The well-defined pits indicate that the etch conditions employed suggest selective etching of GaN over AlGaN. The etch only reveals V-defects, which are filled in during growth without introducing new hexagonal pits from additional threading dislocations or surface defects, making ALE an excellent tool for systematic etch back of LEDs for quick intentional V-defect characterization without the need for growth interrupts or the complexity of a TEM characterization.[27–32] The exposed V-defects are also imaged using SEM in Fig. 2(e), However, due to the removal of the higher doped regions there is significant charging effects, hence ALE followed by AFM is recommended for V-defect characterization. XPS data of the etched surface at 250 etch cycles show 10% Al content, which is only possible if the etch was stopped at the EBL [see Fig. 2(a) inset for the epitaxial structure].

We can characterize the depth of the damage by etching structures containing single quantum wells.[22,33] For the SQW sample, the top UID-GaN was systematically etched toward the quantum well using ALE. Should the QWs be damaged due to the dry etch, we would expect a decrease in photoluminescence (PL) intensity, such as that shown in Fig. 3(a).[22,33] The distance from the QW in the direction of etch (crystal growth) at which the PL intensity decrease is first observed corresponds to the depth of the damage.[22,33] The etch depth was measured using XRD, and the PL spectra were obtain by resonant excitation of the quantum wells using a 375 nm pump laser for different etch depths using ALE. The PL spectra of an unetched reference sample were used to correct for small changes in beam intensity and angles.

As seen in the change in PL intensities plotted in Fig. 3(b), the damage is low for ALE at small etch depths. At 80 nm etch depth corresponding to 20 nm from the quantum well, the PL intensity is unchanged from that of ∼55 nm from the quantum well with a 30% loss in intensity. This implied that from 150 to 200 cycles of ALE there is no accumulated damage due to the additional cycles. Hence, we can conclude that for material quality sensitive devices, the final etched surface should be more than 55 nm away from the damage sensitive layers. For ICP etch using $Cl_2/BCl_3/Ar$, it has been shown that the Cl radical intensity have little effect on the etch damage.[23] This implies that the damage is not due to plasma-induced charging or plasma-induced irradiation.[23,34] This leaves physical damage as the only possible source of damage. The expected penetration depth for the low energy ions at self-bias of 15 V is only ∼1 nm, which is much less than the depth of damage measured. As mentioned, there are many ways for the damage to propagate, either via diffusion, channeling, or secondary collisions.[34–36]

We attempt to quantify the degree of damage due to the etch on typical *p*-doped regions of an LED by measuring the sheet resistance, R_S of the etched regions and the corresponding bulk resistivity using circular transmission line measurements (CTLMs).[37,38] The MDp and HDp samples are subjected to ALE etches, which resulted in 22, 44,

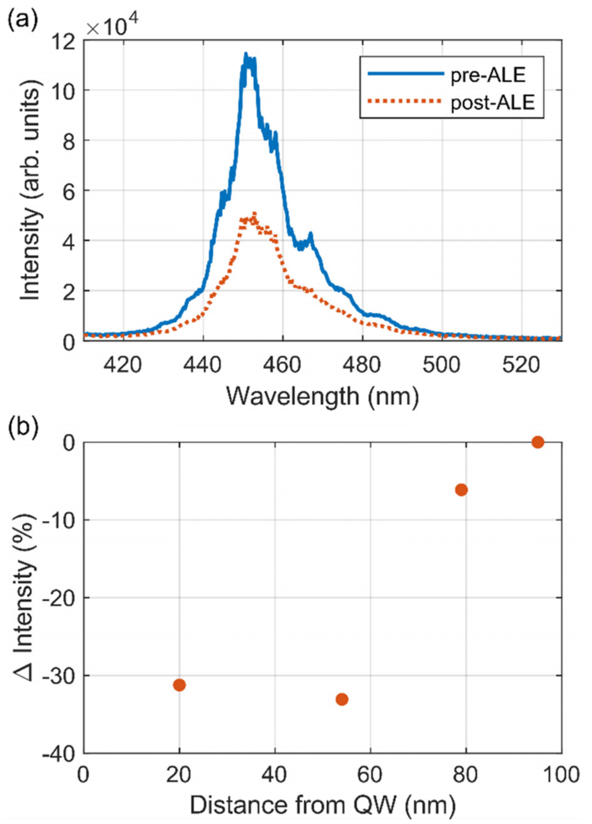

FIG. 3. The PL overall intensity was observed to decrease at 44 nm etch depth (∼55 nm from quantum well) as shown in (a), while the integrated change in intensity of PL is plotted in (b).

and 66 nm etch depth. The *p*-metal contact, 30/300 nm of Pd/Au, was patterned and deposited post-etch. The resistances, R, of the various gap sizes follow the CTLM analytical equation:

$$R = \frac{V_{\text{measured}}}{I_{\text{applied}}} = \frac{R_S}{2\pi}\left[\ln\left(\frac{r_1}{r_0}\right) + \frac{L_T}{r_0}\cdot\frac{I_0\left(\frac{r_0}{L_T}\right)}{I_1\left(\frac{r_0}{L_T}\right)} + \frac{L_T}{r_1}\cdot\frac{K_0\left(\frac{r_1}{L_T}\right)}{K_1\left(\frac{r_1}{L_T}\right)}\right], \tag{1}$$

where I_{applied} and V_{measured} are the applied current and measured voltage (or vice versa); r_0 and r_1 are the inner and outer radii of the CTLM device annulus; L_T is the transfer length of the contact–semiconductor interface; and I_α and K_α are modified Bessel functions of the first and second kind of order α, respectively.[37,39,40] The specific contact resistivity of the interface is hence $\rho_C = R_S {L_T}^2$. While in application the CTLM analytical equation can be applied to any reasonably ohmic contact, it is important to distinguish between an ohmic contact and a Schottky contact. In the latter, the diode contribution will show up as a current barrier. As such, a direct application of the CTLM equation will overestimate the sheet resistance while underestimating the specific contact resistance. Nevertheless, it is still possible to estimate the sheet resistance for any reasonably linear current–voltage curves (I–V), and the trend of bulk resistivity calculated from the sheet resistance with increasing etch depths is expected to be illustrative of the accumulated damage due to the dry etching, if any.

The ohmic nature of the contacts can be represented by their linearity in terms of Pearson's coefficients for linear fits of the current – voltage curves, where a perfectly ohmic contact will have Pearson's coefficient of 1, and a contact is Schottky at Pearson's coefficients less than approximately 0.9. For MDp, we observe Schottky contacts even for the unetched reference [Fig. 4(a)]. That said, the Pearson's coefficients are still fairly close to 0.9, hence we will proceed with estimating the sheet resistances and hence bulk resistivity using the CTLM method. The current–voltage curves remain highly linear for the different gap sizes for HDp with Pearson's coefficient >0.9 for all etch

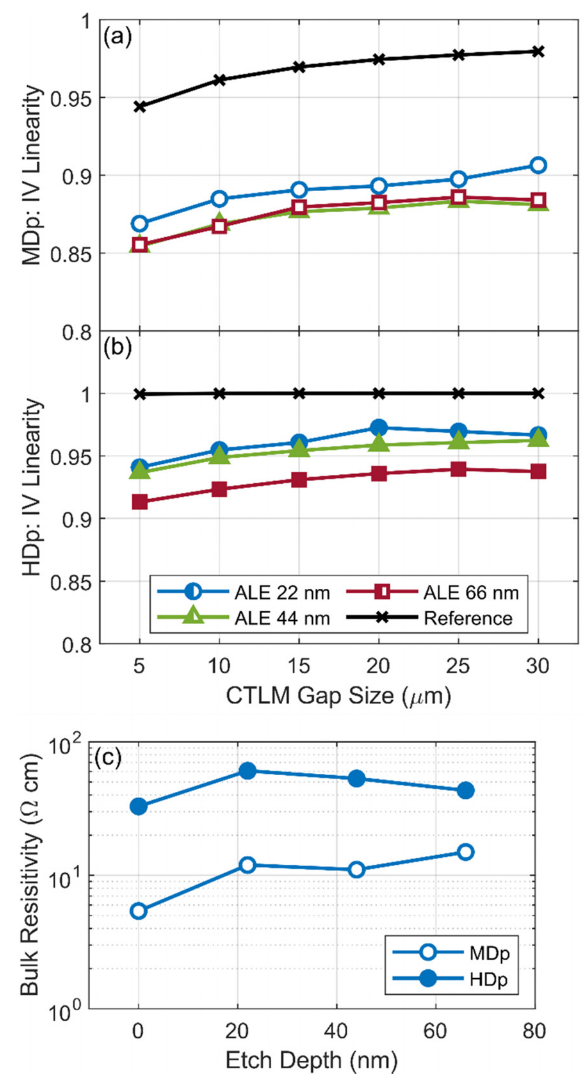

FIG. 4. The linear fit Pearson's coefficients for MDp and HDp are plotted in (a) and (b), respectively. The fitted bulk resistivity for MDp and HDp etched using ALE are plotted in (c). The reference data points in (a) and (b) correspond to the etch depth = 0 nm data in (c). Lines are only to guide the eye.

depths using both etch techniques. In general, the larger gap size devices have higher linearity due to the larger resistance component compared to the diode component of a Schottky contact.

For HDp, the bulk resistivity obtained from the fitted sheet resistances remained unchanged at $\sim$40 Ω cm regardless of etch depth, as shown in Fig. 4(c). This implied that there is little to no damage for ALE as the change to the resistances due to etches are smaller than the variation in fitted sheet resistances of the unetched highly doped material. In contrast, for the MDp samples there was a clear trend with increasing etch depth, where the calculated bulk resistivity increases gradually with increasing etch depth from 5 to 15 Ω cm. The increase is, however, small, indicating very little accumulated damage in the remnant layers with increasing etch depth. Note that the bulk resistivity values for MDp was lower than HDp due to the self-compensating effect of Mg in Mg-doped GaN.[41]

In conclusion, our studies generally indicate while the damage is deep, and the resultant bulk resistivities indicate that the damage is very small, with no significant measured change from 100 to 200 cycles of etches. The finite thickness of damaged region places a lower bound on the remnant *p*-layer thickness in these studies, which can be designed around experimentally. Nevertheless, for surface sensitive devices, a damage recovery step post-etch is highly desirable and should be developed. Morphologically, ALE produced etched surfaces that are smooth, being highly "conformal" with no added roughness due to etch, retaining the step-terrace features of the as-grown surface. The high etch selectivity of ALE for GaN over $Al_{0.1}Ga_{0.9}N$ combined with the smooth etch morphology makes ALE a useful tool to characterize V-defects in nitride LEDs.

We would like to thank Tom Mates for useful guidance on the usage of SIMS and XPS. Support at UCSB was provided by the Solid State Lighting and Energy Electronics Center (SSLEEC); U.S. Department of Energy under the Office of Energy Efficiency & Renewable Energy (EERE) (Award No. DE-EE0009691) and under the Advanced Research Projects Agency – Energy (ARPA-E) (Award No. DE-AR0001591); the Lawrence Livermore National Laboratory – Lab Directed Research and Development (LLNL-LDRD) Program (Project No. 21-ERD-036); the Simons Foundation (Grant No. 601952); the National Science Foundation (NSF) RAISE program (Grant No. DMS-1839077); and Sandia National Laboratory (Award No. 2150283). A portion of this work was performed at the UCSB Nanofabrication facility. The research reported here made use of shared facilities of the UCSB MRSEC (No. NSF DMR 1720256).

AUTHOR DECLARATIONS

Conflict of Interest

The authors have no conflicts to disclose.

Author Contributions

Wan Ying Ho: Conceptualization (lead); Formal analysis (lead); Investigation (lead); Validation (lead); Visualization (lead); Writing – original draft (lead). **James S. Speck:** Formal analysis (supporting); Funding acquisition (lead); Project administration (lead); Resources (supporting); Supervision (lead); Writing – review & editing (equal). **Yi Chao Chow:** Formal analysis (supporting); Investigation (supporting); Resources (equal); Writing – review & editing (equal). **Zachary J. Biegler:** Formal analysis (supporting); Investigation (supporting); Resources (equal); Writing – review & editing (equal). **Kai Shek Qwah:** Investigation (supporting); Resources (equal); Writing – review & editing (equal). **Tanay Tak:** Formal analysis (supporting); Investigation (supporting); Writing – review & editing (equal). **Ashley Wissel-Garcia:** Investigation (supporting); Resources (equal); Writing – review & editing (equal). **Iris Liu:** Investigation (supporting); Writing – review & editing (supporting). **Feng Wu:** Investigation (equal); Writing – review & editing (equal). **Shuji Nakamura:** Resources (equal).

DATA AVAILABILITY

The data that support the findings of this study are available from the corresponding author upon reasonable request.

REFERENCES

[1]D. Zhuang and J. H. Edgar, "Wet etching of GaN, AlN, and SiC: A review," Mater. Sci. Eng. R **48**(1), 1–46 (2005).

[2]D. Li, M. Sumiya, S. Fuke, D. Yang, D. Que, Y. Suzuki, and Y. Fukuda, "Selective etching of GaN polar surface in potassium hydroxide solution studied by x-ray photoelectron spectroscopy," J. Appl. Phys. **90**(8), 4219–4223 (2001).

[3]D. Li, M. Sumiya, K. Yoshimura, Y. Suzuki, Y. Fukuda, and S. Fuke, "Characteristics of the GaN polar surface during an etching process in KOH solution," Phys. Status Solidi A **180**(1), 357–362 (2000).

[4]D. A. Stocker, E. F. Schubert, and J. M. Redwing, "Crystallographic wet chemical etching of GaN," Appl. Phys. Lett. **73**(18), 2654–2656 (1998).

[5]A. C. Tamboli, A. Hirai, S. Nakamura, S. P. DenBaars, and E. L. Hu, "Photoelectrochemical etching of p-type GaN heterostructures," Appl. Phys. Lett. **94**(15), 151113 (2009).

[6]C. Youtsey, I. Adesida, L. T. Romano, and G. Bulman, "Smooth n-type GaN surfaces by photoenhanced wet etching," Appl. Phys. Lett. **72**(5), 560–562 (1998).

[7]C. Y. Chan, S. Namiki, J. K. Hite, M. A. Mastro, S. B. Qadri, and X. Li, "Homoepitaxial GaN micropillar array by plasma-free photo-enhanced metal-assisted chemical etching," J. Vac. Sci. Technol. A **39**(5), 053212 (2021).

[8]Y. Horiike, T. Tanaka, M. Nakano, S. Iseda, H. Sakaue, A. Nagata, H. Shindo, S. Miyazaki, and M. Hirose, "Digital chemical vapor deposition and etching technologies for semiconductor processing," J. Vac. Sci. Technol. A **8**(3), 1844–1850 (1990).

[9]G. C. DeSalvo, C. A. Bozada, J. L. Ebel, D. C. Look, J. P. Barrette, C. L. A. Cerny, R. W. Dettmer, J. K. Gillespie, C. K. Havasy, T. J. Jenkins, K. Nakano, C. I. Pettiford, T. K. Quach, J. S. Sewell, and G. D. Via, "Wet chemical digital etching of GaAs at room temperature," J. Electrochem. Soc. **143**(11), 3652–3656 (1996).

[10]K. Ikeda, S. Imai, and M. Matsumura, "Atomic layer etching of germanium," Appl. Surf. Sci. **112**, 87–91 (1997).

[11]D. Buttari, S. Heikman, S. Keller, and U. K. Mishra, in *Proceedings. IEEE Lester Eastman Conference on High Performance Devices* (IEEE, Newark, DE, USA, 2002), pp. 461–469.

[12]C. Kauppinen, S. A. Khan, J. Sundqvist, D. B. Suyatin, S. Suihkonen, E. I. Kauppinen, and M. Sopanen, "Atomic layer etching of gallium nitride (0001)," J. Vac. Sci. Technol. A **35**(6), 060603 (2017).

[13]H. Fukumizu, M. Sekine, M. Hori, K. Kanomaru, and T. Kikuchi, "Atomic layer etching of AlGaN using Cl_2 and Ar gas chemistry and UV damage evaluation," J. Vac. Sci. Technol. A **37**(2), 021002 (2019).

[14]S. Ruel, P. Pimenta-Barros, F. L. Roux, N. Chauvet, M. Massardier, P. Thoueille, S. Tan, D. Shin, F. Gaucher, and N. Posseme, "Atomic layer etching of GaN using Cl_2 and He or Ar plasma," J. Vac. Sci. Technol. A **39**(2), 022601 (2021).

[15]K. J. Kanarik, T. Lill, E. A. Hudson, S. Sriraman, S. Tan, J. Marks, V. Vahedi, and R. A. Gottscho, "Overview of atomic layer etching in the semiconductor industry," J. Vac. Sci. Technol. A **33**(2), 020802 (2015).

[16]K. J. Kanarik, S. Tan, W. Yang, T. Kim, T. Lill, A. Kabansky, E. A. Hudson, T. Ohba, K. Nojiri, J. Yu, R. Wise, I. L. Berry, Y. Pan, J. Marks, and R. A. Gottscho, "Predicting synergy in atomic layer etching," J. Vac. Sci. Technol. A **35**(5), 05C302 (2017).
[17]J. Iveland, L. Martinelli, J. Peretti, J. S. Speck, and C. Weisbuch, "Direct measurement of auger electrons emitted from a semiconductor light-emitting diode under electrical injection: Identification of the dominant mechanism for efficiency droop," Phys. Rev. Lett. **110**(17), 177406 (2013).
[18]D. J. Myers, A. C. Espenlaub, K. Gelzinyte, E. C. Young, L. Martinelli, J. Peretti, C. Weisbuch, and J. S. Speck, "Evidence for trap-assisted Auger recombination in MBE grown InGaN quantum wells by electron emission spectroscopy," Appl. Phys. Lett. **116**(9), 091102 (2020).
[19]W. Y. Ho, Y. C. Chow, D. J. Myers, F. Wu, J. Peretti, C. Weisbuch, and J. S. Speck, "Quantitative correlation of hot electron emission to Auger recombination in the active region of c-plane blue III-N LEDs," Appl. Phys. Lett. **119**(5), 051105 (2021).
[20]W. Y. Ho, C. W. Johnson, T. Tak, M. Sauty, Y. C. Chow, S. Nakamura, A. Schmid, J. Peretti, C. Weisbuch, and J. S. Speck, "Steady-state junction current distribution in p-n GaN diodes measured using low-energy electron microscopy (LEEM)," Appl. Phys. Lett. **123**(3), 031101 (2023).
[21]M. Dineen, M. Loveday, A. Goodyear, M. Cooke, A. Newton, S. Baclet, C. Ward, and T. Hemakumara, in *Advanced Etch Technology for Nanopatterning IX*, edited by C. B. Labelle and R. S. Wise (SPIE, San Jose, United States, 2020), p. 17.
[22]J. G. Nedy, N. G. Young, K. M. Kelchner, Y. Hu, R. M. Farrell, S. Nakamura, S. P. DenBaars, C. Weisbuch, and J. S. Speck, "Low damage dry etch for III-nitride light emitters," Semicond. Sci. Technol. **30**(8), 085019 (2015).
[23]R. J. Shul, L. Zhang, A. G. Baca, C. G. Willison, J. Han, S. J. Pearton, and F. Ren, "Inductively coupled plasma-induced etch damage of GaN p-n junctions," J. Vac. Sci. Technol. A **18**(4), 1139–1143 (2000).
[24]J. Ladroue, A. Meritan, M. Boufnichel, P. Lefaucheux, P. Ranson, and R. Dussart, "Deep GaN etching by inductively coupled plasma and induced surface defects," J. Vac. Sci. Technol. A **28**(5), 1226–1233 (2010).
[25]A. Pandey, B. S. Yadav, D. V. S. Rao, D. Kaur, and A. K. Kapoor, "Dislocation density investigation on MOCVD-grown GaN epitaxial layers using wet and dry defect selective etching," Appl. Phys. A **122**(6), 614 (2016).
[26]M. Tahhan, J. Nedy, S. H. Chan, C. Lund, H. Li, G. Gupta, S. Keller, and U. Mishra, "Optimization of a chlorine-based deep vertical etch of GaN demonstrating low damage and low roughness," J. Vac. Sci. Technol. A **34**(3), 031303 (2016).
[27]Y. Li, F. Yun, X. Su, S. Liu, W. Ding, and X. Hou, "Carrier injection modulated by V-defects in InGaN/GaN multiple-quantum-well blue LEDs," Jpn. J. Appl. Phys., Part 1 **53**(11), 112103 (2014).
[28]F. Wu, J. Ewing, C. Lynsky, M. Iza, S. Nakamura, S. P. DenBaars, and J. S. Speck, "Structure of V-defects in long wavelength GaN-based light emitting diodes," J. Appl. Phys. **133**(3), 035703 (2023).
[29]Q. Lv, J. Liu, C. Mo, J. Zhang, X. Wu, Q. Wu, and F. Jiang, "Realization of highly efficient InGaN green LEDs with sandwich-like multiple quantum well structure: Role of enhanced interwell carrier transport," ACS Photonics **6**(1), 130–138 (2019).
[30]F. Jiang, J. Zhang, L. Xu, J. Ding, G. Wang, X. Wu, X. Wang, C. Mo, Z. Quan, X. Guo, C. Zheng, S. Pan, and J. Liu, "Efficient InGaN-based yellow-light-emitting diodes," Photonics Res. **7**(2), 144 (2019).
[31]Y. Li, F. Yun, X. Su, S. Liu, W. Ding, and X. Hou, "Deep hole injection assisted by large V-shape pits in InGaN/GaN multiple-quantum-wells blue light-emitting diodes," J. Appl. Phys. **116**(12), 123101 (2014).
[32]C.-K. Li, C.-K. Wu, C.-C. Hsu, L.-S. Lu, H. Li, T.-C. Lu, and Y.-R. Wu, "3D numerical modeling of the carrier transport and radiative efficiency for InGaN/GaN light emitting diodes with V-shaped pits," AIP Adv. **6**(5), 055208 (2016).
[33]J.-M. Lee, C. Huh, D.-J. Kim, and S.-J. Park, "Dry-etch damage and its recovery in InGaN/GaN multi-quantum-well light-emitting diodes," Semicond. Sci. Technol. **18**(6), 530–534 (2003).
[34]K. Eriguchi, "Characterization techniques of ion bombardment damage on electronic devices during plasma processing—plasma process-induced damage," Jpn. J. Appl. Phys., Part 1 **60**(4), 040101 (2021).
[35]S. Tian, M. F. Morris, S. J. Morris, B. Obradovic, G. Wang, A. F. Tasch, and C. M. Snell, "A detailed physical model for ion implant induced damage in silicon," IEEE Trans. Electron Devices **45**(6), 1226–1238 (1998).
[36]H. Yu, U. Peralagu, A. Alian, M. Zhao, B. Parvais, and N. Collaert, "Parasitic side channel formation due to ion implantation isolation of GaN HEMT," MRS Adv. **7**(36), 1274–1278 (2022).
[37]J. H. Klootwijk and C. E. Timmering, in *Proceedings of the 2004 International Conference on Microelectronic Test Structures (IEEE Cat. No.04CH37516)* (IEEE, Awaji Yumebutai, Japan, 2004), pp. 247–252.
[38]Y. Pan, *Versatile Circular Test Structure for Ohmic Contact Characterisation* (Royal Melbourne Institute of Technology (RMIT), 2015).
[39]S. S. Cohen and G. S. Gildenblat, *Metal-Semiconductor Contacts and Devices* (Academic Press, 1986), Vol. 13.
[40]B. Jacobs, M. Kramer, E. J. Geluk, and F. Karouta, "Optimisation of the Ti/Al/Ni/Au ohmic contact on AlGaN/GaN FET structures," J. Cryst. Growth **241**(1–2), 15–18 (2002).
[41]U. Kaufmann, P. Schlotter, H. Obloh, K. Köhler, and M. Maier, "Hole conductivity and compensation in epitaxial GaN:Mg layers," Phys. Rev. B **62**(16), 10867–10872 (2000).